J Mol Model (2013) 19:2525–2538
DOI 10.1007/s00894-013-1807-y

ORIGINAL PAPER

Effects of water content on the tetrahedral intermediate of chymotrypsin - trifluoromethylketone in polar and non-polar media: observations from molecular dynamics simulation

Xue Tian · Lin Jiang · Yuan Yuan · Minqi Wang · Yanzhi Guo · Xiaojun Zeng · Menglong Li · Xuemei Pu

Received: 1 January 2013 / Accepted: 12 February 2013 / Published online: 1 March 2013

Abstract The work uses MD simulation to study effects of five water contents (3 %, 10 %, 20 %, 50 %, 100 %v/v) on the tetrahedral intermediate of chymotrypsin - trifluoromethyl ketone in polar acetonitrile and non-polar hexane media. The water content induced changes in the structure of the intermediate, solvent distribution and H-bonding are analyzed in the two organic media. Our results show that the changes in overall structure of the protein almost display a clear correlation with the water content in hexane media while to some extent U-shaped/bell-shaped dependence on the water content is observed in acetonitrile media with a minimum/maximum at 10–20 % water content. In contrast, the water content change in the two organic solvents does not play an observable role in the stability of catalytic hydrogen-bond network, which still exhibits high stability in all hydration levels, different from observations on the free enzyme system [Zhu L, Yang W, Meng YY, Xiao X, Guo Y, Pu X, Li M (2012) J Phys Chem B 116(10):3292–3304]. In low hydration levels, most water molecules mainly distribute near the protein surface and an increase in the water content could not fully exclude the organic solvent from the protein surface. However, the acetonitrile solvent displays a stronger ability to strip off water molecules from the protein than the hexane. In a summary, the difference in the calculated properties between the two organic solvents is almost significant in low water content (<10 %) and become to be small with increasing water content. In addition, some structural properties at 10~20 %v/v hydration zone, to large extent, approach to those in aqueous solution.

Keywords Molecular dynamics simulation · Organic media · Tetrahedral intermediate of chymotrypsin · Water content

X. Tian · L. Jiang · M. Wang · Y. Guo · X. Zeng · M. Li · X. Pu (✉)
Faculty of Chemistry, Sichuan University, Chengdu 610064, People's Republic of China
e-mail: xmpuscu@scu.edu.cn

Y. Yuan
College of Management, Southwest University for Nationalities, Chengdu 610041, People's Republic of China

Introduction

Enzymatic reaction in aqueous-organic media has attracted worldwide interest since it has many distinctive characteristics compared with that in aqueous environment, such as, lesser side reactions, higher thermal stability, higher solubility for enzyme substrate, and so on [1, 2]. However, low catalytic activity of enzymes presented in the non-aqueous media limits its further applications. Experimental studies have shown that proteins, in order to retain their activity in anhydrous solvents, require some water molecules to be present and also found that the enzyme activity is associated with the water content. Some research works have revealed that low hydration level could lead to a drop of enzyme activity, and conversely, high hydration level could increase the enzyme activity but lose the advantage in organic media [3–12]. Thus, how to control hydration conditions to obtain an optimal activity of enzyme in non-aqueous media becomes pivotal in application. Many experimental efforts have been devoted to explore the correlation between the water content and the enzyme activity. Kijima [13] investigated the correlation between the activity of α-

chymotrypsin and the concentration of water/organic solvent mixtures (10 %–100 %). Partridge [4] discussed the thermodynamic stability and the kinetic stability of α-chymotrypsin in water/acetonitrile solvent mixtures at low water content. The study about secondary structure and enzyme activity of α-chymotrypsin and the trypsin was also carried out in three organic solvents (ethanol, 1,4-dioxane, and acetonitrile) with various hydration levels [14]. These experiment research works showed that the enzyme activity in organic solvents with low concentration is close to that in aqueous solution, and enzyme could maintain its catalytic activity in organic solvents with high concentration. However, the influence mechanism of water content on the enzyme structure and its activity is still disputable. In fact, it is difficult for experiments to probe atomistic details of organic solvent–enzyme–essential water interaction at different hydration levels, and to determine the subtle structure changes in the active site owing to the complexity of the enzyme structure and the molecular nature of the issue. Therefore, more relevant studies and information are needed to understand well the mechanism. Molecular dynamics simulations could provide a molecular level view of the solute-solvent interaction and could reveal dynamic behavior of proteins. The method has been successfully used to study enzymes in aqueous solution [15–18] and non-aqueous media [19–22] to obtain microscopic information at the molecular level and supplement for experimental investigations. Micaêlo [21] used MD to investigate cutinase in five organic solvents with different water contents, and discussed its dynamical properties and distribution of water and organic solvent around protein surface. Yang [23] studied the structure and flexibility of subtilisin in three organic solvents and pure water using MD simulation. Trodler and Pleiss [24] discussed the correlation between enzyme flexibility and the organic solvent through simulating the Candida Antarctica lipase B in aqueous environment and organic solvents. Li Cong [25] analyzed the structure and activity of CALB in six solvents with different polarity using MD simulation and suggested that the activity of enzymes in non-polar solvent is higher than that in polar solvent. Wedberg [26] used MD method to study dynamic properties of CALB in aqueous and four organic solvents with different water contents and predicted its activity changes through calculating free energies. All the results above showed that the water content and organic solvent play a significant role in the enzyme structure and flexibility. However, it should be noted that these previous investigations only focused on the isolated enzyme without any substrates or inhibitors. The observations derived from these works provide valuable information for understanding effects of water content on the enzyme structure, flexibility and some other specific properties at the molecular level. However, they are still limited to gain systematic insight into the effect of water content and organic solvent on the function of enzyme since the enzyme activity is closely associated with substrates and transition state [27, 28]. However, the information concerning enzyme-substrate complex or transition state in non-aqueous media remains elusive.

Serine protease is one of the most used enzyme family. Its catalytic mechanism [29] is generally acid–base catalysis, which depends on three amino acid residues (viz., histidine, aspartate, and serine) and includes acylation and deacylation steps. In the acylation reaction, His57 acts as a general base to accept a proton from hydroxyl of Ser195 and then the Ser195 attacks the carbonyl of the peptide substrate to yield a tetrahedral intermediate, which is the rate-controlling step in the catalytic reaction. The structure of the tetrahedral intermediate is very close to that of the transition state. Thus, the knowledge about the intermediate is important in understanding the catalytic mechanism. However, it is difficult for experiments to obtain directly the information owing to the very short lifetime of the tetrahedral intermediate of the enzyme/substrate. Indeed, the experimental and theoretical knowledge about the intermediate was mainly derived from indirect studies on the tetrahedral intermediates of enzyme-inhibitors or enzyme/substrate-like. For example, some experimental and theoretical works successfully revealed some factors, which influence the enzyme activity in aqueous solution, through analyzing active site of the tetrahedral intermediate [30–35]. However, the information about the intermediate has been absent in non-aqueous enzymatic catalysis, as mentioned above. Thus, we, herein, selected the tetrahedral intermediate of chymotrypsin and trifluoromethylketone as a model of the transition state and used the MD method to study it in polar acetonitrile and non-polar hexane media with different water contents. Our work focused on the effects of the water contents on the overall structure of the enzyme, solvent distribution and hydrogen bonding in the two organic media. The observation derived from the work should provide some new insight added to the previous studies for better understanding the structure and function of enzyme in non-aqueous media.

Computational details

All molecular dynamics simulations were done using AMBER 10.0 program [36]. The AMBER03 force field [37] was used for γ-chymotrypsin, and the TIP3P model [38] was applied to the water molecules. The GAFF force field [39] was utilized for the organic solvent molecules and

trifluoromethylketone, and their atom types were allocated using AMTECHAMBER module [40]. The initial coordinate of the crystallographic tetrahedral intermediate of γ-chymotrypsin - trifluoromethylketone was obtained from Brookhaven Protein Data Bank (its entry code is 6GCH [41]). In the X-ray structure, the enzyme molecule consists of three peptide segments (1–11, 16–146, 151–245) connected by disulfide bonds. The intermediate contains 237 residues and one inhibitor (viz., trifluoromethyl ketone). Five hydration contents (3 %, 10 %, 20 %, 50 %, 100 % (v/v)) were considered in the work. As a reference, the intermediate in pure organic solvents without any water molecule was also studied. In aqueous and organic solutions, we retained all crystal waters (188). Extra water molecules were added on the surface of protein by a solvent shell with certain thickness dependent on the water content and then solvated by acetonitrile or hexane using the XLEAP utility. The rectangle periodic box was set up so that any solute atom is at least 12 Å from any of the box edges for the organic media systems and 10 Å for the aqueous system. Three chloride ions were introduced in order to neutralize the system. To remove bad contacts in the initial geometries of these systems, three energy minimizations (5000 steps for the solvent molecules followed by 5000 steps for the protein and, finally, 5000 steps for the whole system) were done by the same procedure: the steepest descent method for the first 3000 steps for relaxation of the close contacts, followed by conjugate gradient algorithm for the remaining part. After minimizations, the systems were heated gradually from 0 to 300 K within 120 ps. Then, 2 ns dynamic simulations were carried out with periodic boundary conditions in the NVT ensemble at 300 K using the Berendsen temperature coupling [42]. Finally, 8 ns NPT simulation (T=300 K and P=1 atm) was performed. A time step of 2 fs was utilized for all MD simulations. The SHAKE algorithm [43] was utilized for constraining all the bonds involving a hydrogen atom with a tolerance of 1.0×10^{-5} Å. Non-bond interactions were handled with a 12 Å atom-based cutoff. Particle-Mesh-Ewald (PME) method [44, 45] was applied to handle the long-range electrostatic interactions. The last 2 ns trajectory was saved every 1 ps for analysis. All of the MD results were analyzed, using analysis module of AMBER 10.0 and some other developed specific trajectory analysis software.

Results and discussion

RMSD and RMSF values of the enzyme

The root-mean-square deviation (RMSD) is usually used to compare the deviation between the structure of a dynamic protein and the structure of its native state and can be calculated in terms of Eq. 1.

$$RMSD(v,w) = \sqrt{\frac{1}{n}\sum_{i=1}^{n}(v_i - w_i)^2} = \sqrt{\frac{1}{n}\sum_{i=1}^{n}\left((v_{ix} - w_{ix})^2 + (v_{iy} - w_{iy})^2 + (v_{iz} - w_{iz})^2\right)} \quad (1)$$

Where v and w denote the two proteins and n denotes the number of atoms of the protein. Herein, the RMSD is for the deviation from the crystal structure of the protein in aqueous solution. The averaged RMSD values over the last 2 ns trajectories are calculated and listed in Table 1. As shown in the Fig. 1, the RMSD of the enzyme in hexane medium decreases with increasing water content. However, the RMSD values in the acetonitrile medium do not display such a clear variation trend as the non-polar hexane medium. For acetonitrile medium, the RMSD value at 20 % hydration level is close to that at 10 % level and both values are smaller than those at the other hydration levels (including 50 % water content) but still larger than that in aqueous solution. The RMSD change in the acetonitrile medium seems to display U-shaped dependence on the water content since the RMSD value is minimized at the hydration level of 10–20 % and it becomes larger at the other water contents (either lower or higher than 10–20 % water content), as shown in Fig. 1. The U-shaped dependence of the structure variation on the water content was observed for the RMSD value of free lipase in nonpolar solvent (*tert*-butyl alcohol, MTBE) [26]. Interestingly, the U-shaped dependence in our work is observed in the polar solvent rather than non-polar solvent. This difference suggests that the correlation of the protein structure with the water content also depends on the type of protein, and the inhibitor may, to some extent, play a role in influencing the correlation. The U-shaped dependence of the RMSD on the water content could partly rationalize some experimental findings that some enzyme activities or enantioselectivities are maximized at a specific hydration level (called a bell-shaped dependence) [46, 47].

Compared to hexane medium, the RMSD values in acetonitrile solvent are smaller at the same hydration level. In order to provide a visual view for the solvent induced conformation deviation from the crystal structure, Fig. 2 presents a superimposition of the crystal structure and the average structures of the enzyme in aqueous solution and the two organic media. The average structures in Fig. 2 come from 1000 snapshots taken on the last 2 ns trajectory at 2 ps interval. In Fig. 2, only 0 % (viz., pure organic solvent) and 3 % water contents are selected as representatives of the two organic media. We take the average

Table 1 The RMSD and RMSF values of the enzyme, active residues, inhibitor trifluoromethyl ketone (labeled as APF246) over the last 2 ns trajectories (Å) and their standard deviation [a]

Water content		100 %	50 %	20 %	10 %	3 %	0 %
		RMSD					
All atom	ACN	2.26±0.05	2.42±0.05	2.35±0.06	2.33±0.06	2.42±0.60	2.63±0.07
	HEX	2.26±0.05	2.38±0.08	2.47±0.08	2.53±0.06	2.59±0.03	3.07±0.03
Backbone	ACN	1.54±0.08	1.69±0.06	1.53±0.07	1.49±0.08	1.55±0.06	1.87±0.07
	HEX	1.54±0.08	1.64±0.08	1.71±0.09	1.82±0.07	1.90±0.05	2.16±0.03
APF246	ACN	0.70±0.13	0.97±0.09	0.74±0.14	0.96±0.10	0.95±0.10	0.62±0.14
	HEX	0.70±0.13	0.69±0.15	0.78±0.13	0.93±0.10	0.93±0.09	0.58±0.14
HIS57	ACN	0.28±0.07	0.25±0.06	0.23±0.05	0.25±0.06	0.24±0.06	0.30±0.06
	HEX	0.28±0.07	0.24±0.06	0.23±0.05	0.27±0.07	0.28±0.07	0.25±0.06
SER195	ACN	0.17±0.04	0.14±0.04	0.14±0.04	0.16±0.04	0.13±0.03	0.21±0.05
	HEX	0.17±0.04	0.14±0.04	0.15±0.04	0.14±0.04	0.16±0.04	0.20±0.05
ASP102	ACN	0.25±0.07	0.24±0.06	0.22±0.06	0.22±0.06	0.23±0.06	0.20±0.05
	HEX	0.25±0.07	0.23±0.06	0.20±0.05	0.24±0.06	0.22±0.06	0.26±0.07
		RMSF					
All atom	ACN	0.90±0.11	0.84±0.06	0.72±0.06	0.84±0.07	0.83±0.05	0.81±0.06
	HEX	0.90±0.11	0.89±0.07	0.89±0.10	0.89±0.05	0.71±0.04	0.68±0.05
Backbone	ACN	0.58±0.02	0.54±0.04	0.48±0.03	0.56±0.03	0.53±0.02	0.52±0.02
	HEX	0.58±0.02	0.58±0.05	0.57±0.03	0.57±0.03	0.48±0.02	0.44±0.02
APF246	ACN	0.42±0.06	0.47±0.10	0.44±0.05	0.42±0.05	0.41±0.05	0.41±0.05
	HEX	0.42±0.06	0.50±0.06	0.42±0.05	0.44±0.05	0.41±0.05	0.40±0.04
HIS57	ACN	0.16±0.05	0.17±0.04	0.16±0.04	0.17±0.05	0.16±0.04	0.16±0.04
	HEX	0.16±0.05	0.30±0.03	0.17±0.05	0.19±0.04	0.16±0.05	0.16±0.04
SER195	ACN	0.10±0.03	0.12±0.02	0.11±0.02	0.11±0.03	0.10±0.03	0.10±0.03
	HEX	0.10±0.03	0.19±0.02	0.11±0.03	0.14±0.02	0.10±0.03	0.11±0.03
ASP102	ACN	0.14±0.04	0.16±0.04	0.15±0.04	0.14±0.04	0.14±0.04	0.14±0.04
	HEX	0.14±0.04	0.23±0.03	0.15±0.04	0.17±0.03	0.15±0.04	0.15±0.04

[a] *ACN* denotes acetonitrile media, *HEX* denotes hexane media

structure into account since it may be more representative of what can be observed experimentally by NMR or crystallography. An inspection of Fig. 2a and b shows that there is larger structure deviation from the crystal in hexane medium than that in acetonitrile. This phenomenon is especially apparent in pure organic media without any water molecule (see Fig. 2b), where the protein is significantly compressed toward the inside with respect to those in pure acetonitrile

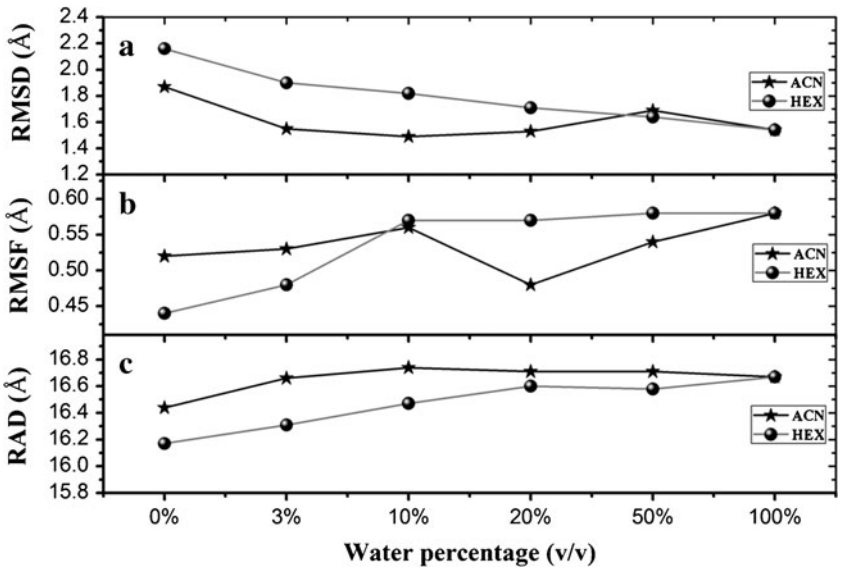

Fig. 1 The correlations of RMSD and RMSF of backbone atoms of the enzyme, and radius of gyration (RAD) of the enzyme with the water contents. ACN denotes acetonitrile media. HEX denotes hexane media

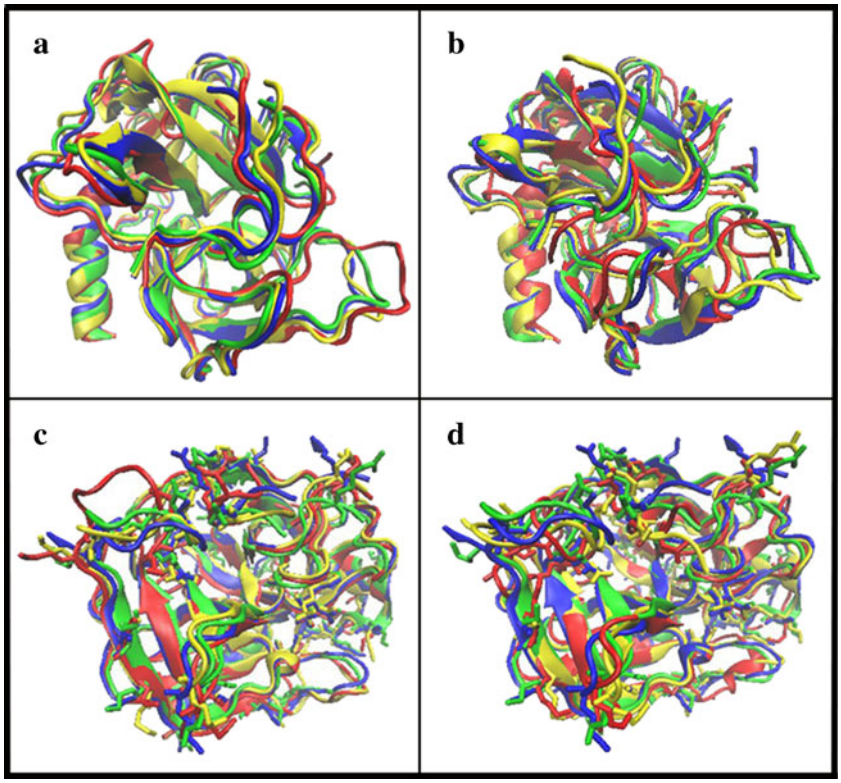

Fig. 2 The superimposition of the averaged structures of chymotrypsins in aqueous (*blue*), hexane (*red*) and acetonitrile (*yellow*) media over the last 2 ns trajectories. The crystal structure (*green*) of the enzyme is employed as a reference in all cases. The protein structures are drawn based on the second structure. The charged residues are further shown as stick (**c**, **d**). The 3 % (**a**, **c**) and the 0 % (**b**, **d**) water contents are selected as representatives in organic media

and aqueous solutions. The variation trend is not surprising. Indeed, there are 31 charged residues located outside the enzyme (see Fig. 2c and d), which should be sensitive to the changes in solvent composition and favor a polar medium. As illustrated in Fig. 2c and d, some significant rearrangement occurs to many charged residues and some uncharged ones in organic solvents, and the sidechains of those residues reorientate toward the inside to greater extent in pure hexane medium than in pure acetonitrile medium in order to reduce the internal energy of the system. The behavior should contribute to the observation that there are larger RMSD values in neat hexane media than those in neat acetonitrile media. A careful comparison of Fig. 2c with Fig. 2d further shows that the rearrangement of the charged residues presents to a lesser extent in the organic media with 3 % water content than the neat organic media, implying the importance of the essential water.

On the whole, the RMSD result suggests that the non-polar solvent could cause greater structure changes than the polar solvent, consistent with the previous observation derived from free lipase in six organic solvents [25], which suggested that its RMSD values increase as the polarity of the solvents decreases. In that study, the RMSD of the lipase increases as the solvent polarity decreases. In addition, the total RMSD values of enzyme are larger in neat acetonitrile and hexane media than in those hydrated by various water contents. This observation suggests the importance of the water in stabilizing the protein structure in non-aqueous media, consistent with results from our previous work [48] on free chymotrypsin in acetonitrile medium, which indicated that the crystal waters in organic media play an important role in preserving native protein structure and some properties associated with the catalytic activity.

The root-mean-square fluctuation (RMSF) is a measure of the deviation between the position of particle i and some reference position, as defined by the Eq. 2.

$$\mathrm{RMSF} = \frac{1}{T}\sum_{t_j=1}^{T}\left(x_i(t_j) - \widetilde{x}_i\right)^2 \tag{2}$$

Where T is the time over which one wants to average, and $\widetilde{x}_i$ is the reference position of particle i. Typically, this reference position will be the time-averaged position of the same particle i, which is considered as the average coordinate over the last 2 ns trajectories in the work. The RMSF about the averaged equilibrium conformation often serves as an indicator to estimate flexibility of protein, which was suggested to be a character related with the protein activity [23, 25]. Both Table 1 and Fig. 1 show the calculated RMSF values of the protein and some important residues at different water content levels. Data in Table 1 shows that the RMSF values of the proteases in the hexane medium increase with increasing water content and become almost constant at higher than 10 % water content. Similar to the RMSD variation, the RMSF values in acetonitrile medium do not present a clear correlation with the water content but

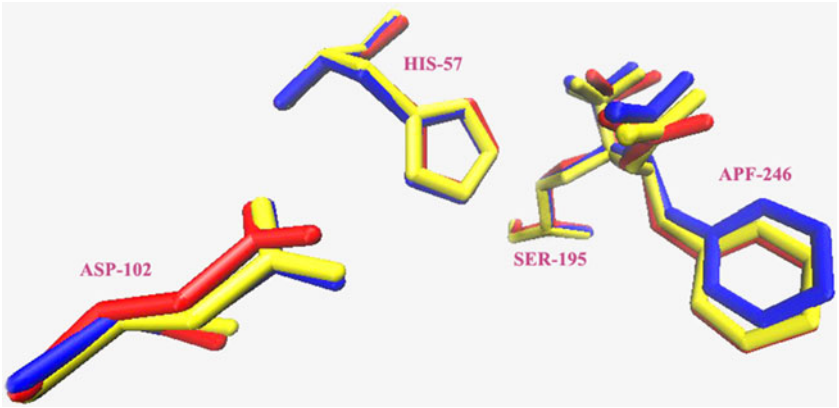

Fig. 3 The superimposition of the averaged structures of three catalytic residues (viz., His57, Asp102 and Ser195) and the inhibitor trifluoromethylketone (APF246) over the last 2 ns trajectories in aqueous solution (*blue*), hexane media with 3 % water content (*red*) and acetonitrile media with 3 % water content (*yellow*). Hydrogen atoms are not shown

display to some extent U-shaped dependence on the water content with a minimum value at about 20 % water content, as illustrated by Fig. 1.

In addition, we also calculate the average RMSD and RMSF values of the three catalytic residues (His57, Ser195, Asp102) and the inhibitor (viz., trifluoromethylketone). As can be seen from Table 1, the RMSD and RMSF values of the three active residues and trifluoromethylketone are much smaller than those of the total protein at all hydration levels, suggesting the relative rigidity of the catalytic residues. Figure 3 representatively presents a superimposition of the average structure of the three catalytic residues (viz., His57, Asp102 and Ser195) and the inhibitor in aqueous solution and the two organic media with 3 % water content. It can be seen from Fig. 3 that there are only minor displacements for the active residues and the inhibitor between the three media, further displaying the relative rigidity of the active site. MD simulations on free chymotrypsin in aqueous solution, acetonitrile medium [48] and acyl-chymotrypsin in aqueous solution [49] also found that the active site residues present smaller fluctuations than the rest of the protein. The relative rigidity of the active site implies a possibility that enzyme could retain activity in these hydration conditions.

Gyration radius

Gyration radius is the RMS distance of each atom to their centroid [50], and can be used to characterize the variation of overall structure of proteases induced by the solvent and the water content. Table 2 lists the gyration radius of proteases calculated over the last 2 ns simulation. It can be seen that the radius of gyrations are almost 16 Å in the two media with different water contents, showing that there are no significant changes in the overall structure of the protein for these solvent compositions. Figure 1 also reveals the correlation between the gyration radius and the water content in the two media. It is clear that the radius of gyration in acetonitrile medium is slightly higher than that in hexane medium at the same water content level, indicating that the structures of proteases in the hexane solvent are more compact than those in the acetonitrile solvent, which may be attributed to greater rearrangement of hydrophilic residues toward the inside induced by the non-polar media rather

Table 2 Summary of radius of gyration (RAD), SASA, hydrophobic (or hydrophilic) exposed SASA, the number of intra-protein hydrogen bonds (HB), salt bridges (SB) and their standard deviations in acetontrile (ACN) and hexane (HEX) media with different water contents over the last 2 ns simulation

Water contents		100 %	50 %	20 %	10 %	3 %	0 %
RAD (Å)	ACN	16.67±0.05	16.71±0.04	16.71±0.04	16.74±0.04	16.66±0.03	16.44±0.03
	HEX	16.67±0.05	16.58±0.04	16.60±0.04	16.47±0.03	16.31±0.03	16.17±0.03
SASA ($\times 10^3$ Å^2)	ACN	11.36±0.15	11.38±0.15	11.64±0.13	11.45±0.14	11.23±0.12	10.85±0.11
	HEX	11.36±0.15	11.26±0.12	11.17±0.13	10.88±0.12	9.88±0.09	9.56±0.08
Hydrophobic%	ACN	25.45±0.23	27.22±0.13	28.00±0.21	29.27±0.22	28.96±0.25	29.95±0.26
	HEX	25.45±0.23	26.92±0.20	26.48±0.22	27.03±0.24	29.00±0.23	33.17±0.26
Hydrophilic%	ACN	74.55±0.44	72.78±0.43	72.00±0.57	70.73±0.54	71.04±0.45	70.05±0.46
	HEX	74.55±0.44	73.08±0.51	73.52±0.40	72.97±0.48	71.00±0.47	66.83±0.42
HB	ACN	182±6	192±6	196±6	197±6	211±6	249±5
	HEX	182±6	190±6	186±5	192±6	230±6	300±7
SB	ACN	2±1	3±1	4±1	3±1	10±1	14±1
	HEX	2±1	6±2	7±2	7±2	13±1	15±1

than the polar. The most compact structures revealed by the smallest gyration radii are observed in the neat organic solvents relative to these systems hydrated, which are 16.44 Å and 16.17 Å in the neat acetonitrile and hexane media, respectively. As shown in Fig. 1, the differences of gyration radii between the two organic solvents at low hydration levels (< 20 %) are greater than those in high water content (≥ 20 %). The effect of water content on the gyration radius of the enzyme is reduced when the water percentage exceeds 10 %, as shown in Fig. 1.

In addition, we also calculate the number of intra-protein hydrogen bonds (HB) and salt bridges (SB) (see Table 2). The number of the intra-protein interaction is the highest in pure organic solvent due to lack of water molecules, resulting in the smallest radius of gyration. In the level of micro-hydration (viz., 3 % water content, which only contain 188 crystal waters), the numbers of intra-protein salt bridges and HBs are much more than those in higher hydration levels. In general, the number of these interactions displays a drop with increasing water content when the water content is lower than 20 %, after which continuous increase in the water content has much less effect on the number of these intra-protein interactions in the two organic media. In comparison of the polar and non-polar solvents, the number of HB in hexane medium is greater than that in acetonitrile system only when the water content is lower than 10 % while the number of SB is almost higher in hexane media than that in acetonitrile at all the hydration levels.

Solvent accessible surface area (SASA)

Solvent accessible surface area (SASA) can be considered to be an indicator of how the different parts of a protein can interact with each other and be affected by the medium. Thus, we calculate the SASA [51] using the VMD program [52], defined by rolling a probe of given size (1.4 Å) around a van der Waals surface of the protein. Table 2 lists the total SASA values and the percentages of hydrophilic SASA and hydrophobic SASA over the last 2 ns simulation in the two media with different hydration levels. The result shows that the total SASA value increases with increasing water content in hexane medium, consistent with the gyration radius variation values. It is not unexpected since the increase in the gyration radius should be a consequence of looser structure of protein, thus resulting in a rise in the SASA. A significant increase in the SASA value is observed in the water content range from 0 % to 10 %, after which the increasing extent in the SASA induced by the increasing water content become small. When the water content is higher than 50 %, the SASA approaches to the value obtained in aqueous solution. Similar to the RMSD and RMSF variations in acetonitrile medium, the total SASA values in this medium do not display similar dependence to the hexane medium. When the water content is lower than 20 % in acetonitrile medium, an increase in the water content would cause a rise in the total SASA values. However, at higher water content level than 20 %, a continuous increase in the water content resulted conversely in a drop of the SASA value. The total SASA variation trend in the acetonitrile medium displays a bell-like dependence on the water content (see Fig. 4) since it is maximized at about 20 % hydration level and becomes smaller at the other water contents (either higher or lower water contents than 20 %). In comparison of the two organic media, the SASA values of the protein in the hexane medium are lower than those in acetonitrile for all hydration levels, as a consequence of more compact structure in hexane medium than acetonitrile.

To gain further observations about SASA of residues, we focus on SASA variations of hydrophobic and hydrophilic

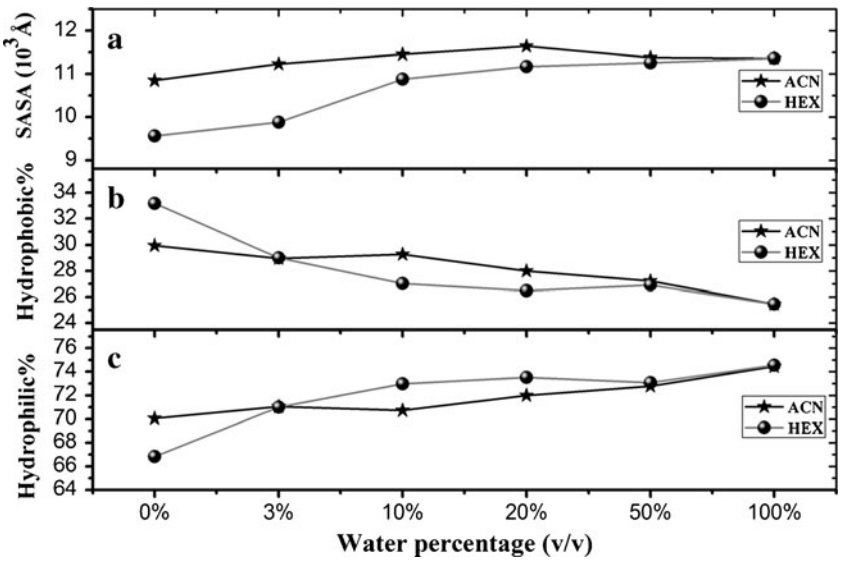

Fig. 4 Correlations of solvent accessible surface area (SASA, 10^3 Å^2) (**a**), hydrophobic (**b**) and hydrophilic (**c**) SASA (%) of the enzyme with water contents. ACN denotes acetonitrile media. HEX denotes hexane media

residues with increasing hydration level. The percentages of hydrophobic SASA and hydrophilic SASA relative to the total SASA (SASA %) are calculated at all hydration levels. The results are listed in Table 2 and shown in Fig. 4. There are obvious correlations between the percentages and the water content. In the two organic solvents, the hydrophilic SASA presents a rising trend with increasing water content while an opposite trend is observed for the hydrophobic SASA.

H-bond analysis in the active site

Since the HB network in active region plays an important role in enzyme catalytic reaction [29, 34], we analyze the hydrogen bonding between the three catalytic residues (viz., Ser195, His57, Asp102), trifluoromethylketone (Apf246) and the solvent molecules at all hydration levels. It is noted that the criteria used for a hydrogen bond in the MD part are solely geometric. The hydrogen bonding is considered to be present if the distance between hydrogen-bonding acceptor and hydrogen-bond donor is less than 3.5 Å and meanwhile, the angle between any two of hydrogen-bonding acceptor atoms, hydrogen atoms or hydrogen-bond donor atoms is greater than 120°. A hydrogen bond is considered to be stable if it exists over more than 90 % of the trajectory time. Table 3 lists the hydrogen bonding between the active residues and trifluoromethylketone in the last 2 ns simulation.

As shown in Table 3, the hydrogen bonding of NE2@His57…OG@Ser195 and OD1@Asp102…ND1@His57 exists for more than 99 % simulation time at all hydration levels. It implies that the two hydrogen bonds are very stable, insensitive to the changes in the type of organic solvent and the water content. The observation is different from the free enzyme system [48], in which the hydrogen bond between the Asp102 and the His57 residues is very stable in acetonitrile medium and aqueous solution but the H-bond between the His57 and Ser195 residue is broken over most of the simulation time. The stable H-bonds in the intermediate system imply possibility of catalytic activity at different hydration levels. Although the two H-bonds are very stable in the two organic media with different hydration levels, the solvent type and water content should influence their strength, judged from the different H-bond distances presented in these systems. However, we can not obtain a clear correlation between the H-bond strength and the water content in the MD work. High level computation should be needed to further address the question.

The experimental study on the structure of chymotrypsin-trifluoromethyl ketone inhibitor complex in aqueous solution [41] already revealed that there is strong H-bonding between the trifluoromethyl ketone inhibitor and Ser195/Gly193 in aqueous solution, which favors stabilization of the tetrahedral intermediate. Thereby, we analyzed the hydrogen bonding between oxygen atoms of trifluoromethyl ketone and the Ser195/Gly193 residues. As shown in Table 3, the hydrogen-bonds of O2@Apf246…N@Ser195 and O2@Apf246…N@Gly193 exists over almost 100 % simulation time in the two media at all hydration levels, displaying high stability. Similarly, the water content should influence the strength of the H-bonds since these H-bond distances are different with varying water

Table 3 Percentage occupation (%) of hydrogen bonds in the active site/their average distances (in Å) in acetonitrile (ACN) and hexane (HEX) media with different water contents [a]

Water content		100 %	50 %	20 %	10 %	3 %	0 %
NE2@His57-OG@Ser195	ACN	100/2.820	99.9/2.883	100/2.837	100/2.845	100/2.833	100/2.814
	HEX	100/2.820	100/2.847	100/2.850	100/2.838	99.9/2.792	99.9/2.785
OD1@Asp102-ND1@His57	ACN	99.7/2.843	100/2.880	99.8/2.79	99.8/2.79	99.8/2.791	99.8/2.77
	HEX	99.7/2.843	99.9/2.837	100/2.807	99.6/2.844	99.5/2.803	100/2.846
OD2@Asp102-ND1@His57	ACN	98.9/3.000	90.01/3.141	84.22/3.197	88.81/3.162	91.51/3.147	76.62/3.21
	HEX	98.9/3.000	93.81/3.113	73.43/3.256	96/3.083	87.01/3.171	78.72/3.19
O@Ser214-N1@Apf246	ACN	60.74/3.213	0	2.5/3.412	21.58/3.308	5.09/3.382	87.01/3.16
	HEX	60.47/3.213	19.68/3.304	3.5/3.337	68.33/3.198	59.04/3.213	91.91/3.10
O2@Apf246-N@Ser195	ACN	100/2.881	99.9/2.811	100/2.807	100/2.791	100/2.766	100/2.804
	HEX	100/2.881	100/2.866	100/2.803	100/2.85	100/2.812	100/2.751
O2@Apf246-N@Ser193	ACN	99.9/2.883	100/2.874	100/2.903	99.8/2.845	99.9/2.92	100/2.783
	HEX	99.9/2.883	98.5/2.988	100/2.880	97.4/2.949	100/2.782	100/2.749

[a] OG@Ser195 denotes OG atom of Ser195 residue. NE2@His57 and ND1@His57 denote NE2 and ND1 atoms of His57 residue, respectively. OD1@Asp102 and OD2@Asp102 denote OD1 and OD2 atoms of Asp102 residue, respectively. N@Ser195 and N@Ser193 denote N atoms of Ser195 and Ser193 residues, respectively. O@Ser214 denotes O atom of Ser214 residue. O2@Apf246 denotes O2 atom of inhibitor trifluoromethyl ketone

Table 4 Percentage occupation (%) of H-bonds between the solvent penetrated into the active site and inhibitor trifluoromethyl ketone (labeled as Apf246) in acetonitrile (ACN) and hexane (HEX) with different water contents over the last 2 ns simulation[a, b, c]

Water contents		100 %	50 %	20 %	10 %	3 %
O2@Apf246-O@WAT	ACN	91	104	192	23	97
	HEX	91	123	103	116	95
F@Apf246-O@WAT	ACN	137	96	53	13	20
	HEX	137	175	245	180	34

[a] O2@Apf246 denotes O2 atom of inhibitor trifluoromethyl ketone

[b] F@Apf246 denotes F atom of inhibitor trifluoromethyl ketone

[c] O@WAT denotes O atom of water molecule

content. Although so, the H-bond distances calculated also do not display a clear correlation with the water content. The H-bonding of O@Ser214…N1@Apf246 was also reported by the experiment [41]. However, the simulation result shows that the H-bond is not as far stable as the H-bonds of O2@Apf246…N@Ser195 and O2@Apf246…N@Gly193. The H-bond has relatively high time occupancy only in neat organic solvent compared to the other solvent compositions, implying that it should be destabilized by the existence of water.

In addition, we also analyze the H-bonding between the solvent molecules penetrated into the active site and some important residues, as listed in Table 4. The result shows that there is nearly no H-bonding between the water molecules and the three catalytic residues (the life time is less than 1 %, so not listed in Table 4). However, there is stable hydrogen bonding between the water molecule and carbonyl oxygen atom of trifluoromethyl ketone since it exists over more than 90 % simulation time in the two media with different hydration levels, suggesting its insensitivity to the organic solvent and the water content. The observation above already indicates that the carbonyl oxygen atom of trifluoromethyl ketone could form stable H-bond with the N-H bond of the Ser195 residues at all hydration levels. Thus, it can be drawn that the carbonyl oxygen atom of trifluoromethyl ketone simultaneously forms H-bond with one water molecule and the Ser195 residue, which should stabilize the tetrahedral intermediate. The water content and the polarity of organic solvent have a minor role in the existence of the H-bond. In addition, it can be observed that one water molecule residing in the active site forms H-bond with the F atom of trifluoromethyl ketone, consistent with the experimental observation [41]. Furthermore, our results also show that the H-bond has high life-time at>3 % water content levels.

On the other hand, we also analyze the H-bonding between the organic solvent molecule and these active residues. The result shows that there is no H-bonding (data is not shown), different from the observation derived from the previous free chymotrypsin in the acetonitrile solvent with 3 % water content [48], which showed that the acetonitrile molecule penetrating into the active site could form H-bond with the active residues. In order to gain insight into this phenomenon, we calculate the number of solvent molecules in the active region (listed in Table 5), defined by 5 Å distance from the OG@Ser195 atom. The result shows that there is nearly no organic solvent penetrating into the active site, especially in hexane medium with more than 10 % water content. Whereas there is at least one water molecule penetrating into the active site in the two organic media with different hydration levels. In acetonitrile medium with 3 % water content, the number of acetonitrile molecules (see Table 5) residing in the active site in the tetrahedral intermediate system is significantly less than that of the free chymotrypsin system [48], where there are about five acetonitrile molecules penetrating into the active site. The difference suggests that the inhibitor would prevent the solvent molecule from penetrating into the active site. Furthermore, we calculate the distance between the active residues (viz., OG@Ser195, OD1@Asp102, OD2@Asp102) and their

Table 5 Number of water molecules and organic molecules within 2.5 Å region from protein surface and in the active region (defined by 5 Å distance from oxygen of Ser195) and their standard deviations in acetonitrile (ACN) and hexane (HEX) with different water contents over the last 2 ns simulation

Water contents		100 %	50 %	20 %	10 %	3 %	0 %
No. of molecules around the protein surface (2.5 Å)							
Water molecule	ACN	492.4±11.9	336.2±14.7	290.2±12.0	220.1±8.7	113.1±4.6	/
	HEX	492.4±11.9	437.8±10.9	424.3±10.8	384.3±10.5	174.0±3.3	/
Organic molecule	ACN	/	72.0±7.3	98.1±8.0	125.7±8.3	164.6±8.5	194.5±8.4
	HEX	/	24.3±3.5	34.0±4.1	46.5±5.1	105.6±5.7	131.5±5.9
No. of molecules in the active site(5 Å)							
Water molecule	ACN	1.3±0.6	2.4±0.6	1.1±0.3	0.3±0.5	1.1±0.2	0
	HEX	1.3±0.6	2.1±0.9	1.9±0.8	2.1±0.8	1.0±0.2	0
Organic molecule	ACN	0	0.3±0.5	0.4±0.6	1.3±0.7	0.6±0.7	0.7±0.7
	HEX	0	0	0	0	0.4±0.5	0.3±0.5

nearest oxygen atoms of water molecules. The result shows that these distances are larger than 3.5 Å. As a consequence, these solvent molecules could not form H-bond with the catalytic residues. It is the absence of the perturbation of solvent molecules in the active site that contributes to high stability in the H-bond network of these catalytic residues. Whereas, there are a few water molecules penetrating into the active site in the free enzyme system and they could form H-bond with the active residues, thus, significantly weakening the stability of the H-bond between the Ser195 and His57 residues, as confirmed by our previous work [48].

In addition, we also analyze the hydrogen bonding between the solvent molecule and N-H@Gly193 and N-H@Ser195 of the oxyanion hole. The result shows that there is no H-bonding between the organic solvent and the two residues since the organic solvent hardly penetrates into the region. Although it is observed that a few water molecules could penetrate into the region, the nearest water molecules to the N-H@Gly193 and N-H@Ser195 locate almost more than 3.5 Å distance from the two groups. As a result, there is nearly no H-bond formed between the water molecule and the oxygen atom, but on occasion H-bonding existed with life time less than 10 %. The observation is also different from the free enzyme system [48], where water and acetonitrile molecules could penetrate into the oxyanion hole and can form stable HBs with the Gly193 residue. Further analysis reveals that the N-H@Gly193 and N-H@Ser195 could form relatively stable H-bond with the inhibitor, which significantly influences the formation of the H-bond between the water molecule and the oxyanion hole (viz., N-H@Gly193 and N-H@Ser195).

Solvent distribution around protein

The enzyme hydration plays an important role in the structure and function of protein. It is revealed that the water molecules closely bound with the protein significantly affect the structure and dynamical property of enzyme in non-aqueous media. To gain insight into the distribution of water around protein surface, we calculate the number of water molecules within 2.5 Å region from the protein surface in respectively aqueous solution and two organic media with different water contents (see Table 5). We focus on the 2.5 Å region since some research works [21] suggested that it is the first hydration shell directly interacting with protein. Figure 5 further displays the correlation between the number of solvents within the 2.5 Å region and the water content. It is apparent that the number of water molecules gradually increase as the water content increases while the number of organic molecule displays an opposite trend. In all hydration levels, the number of water molecules within the 2.5 Å region is greater in hexane medium than that in acetonitrile, indicating that the acetonitrile solvent has stronger ability to strip off water molecules from the protein surface.

To visually view the distributions of the water and the organic solvent molecules around the protein, we select the 3 % water content as a representative to calculate spatial probability density distribution of the solvent molecules on the basis of the last 2 ns trajectories. The average densities of the bulk water, acetonitrile and hexane are calculated to be 0.03344, 0.0116 and 0.0046 atoms/Å ^{3}, respectively. The cutoff values of contour level shown in Fig. 6 are 5, 14 and 36 times higher than the average density of bulk water, acetonitrile and hexane solvents, respectively, which could provide a clear picture for viewing the solvent distributions around the protein. As illustrated by Fig. 6, the spatial contours enclosing high probability regions of the water molecules of the 3 % water content mainly locates on the protein surface and a fraction in the protein interior, not diffusing into the bulk organic solvent. A comparison of Fig. 6a with Fig. 6b indicates that the water molecules around protein surface is significantly more in hexane media

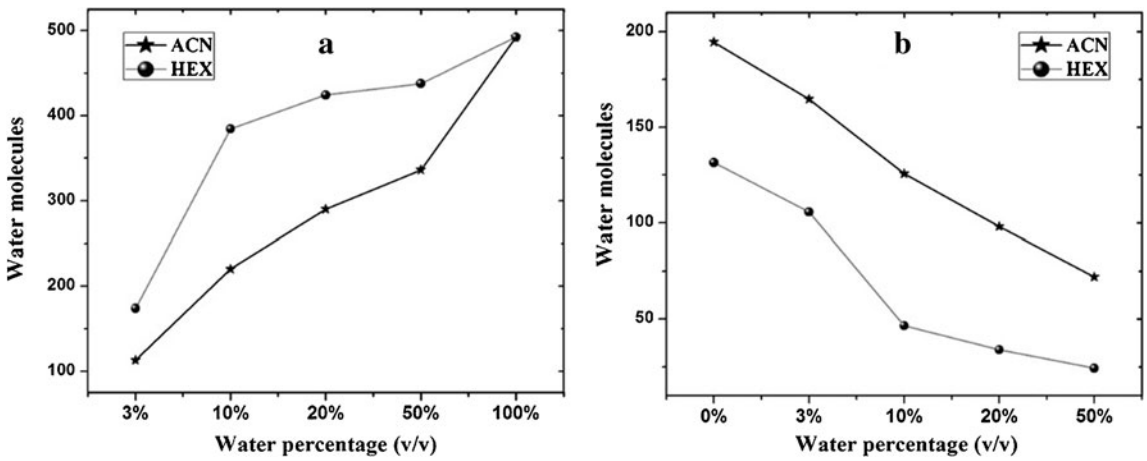

Fig. 5 The correlations of the number of water molecules (**a**) and organic molecules (**b**) within 2.5 Å region from protein surface with water contents in acetonitrile (ACN) and hexane (HEX) media

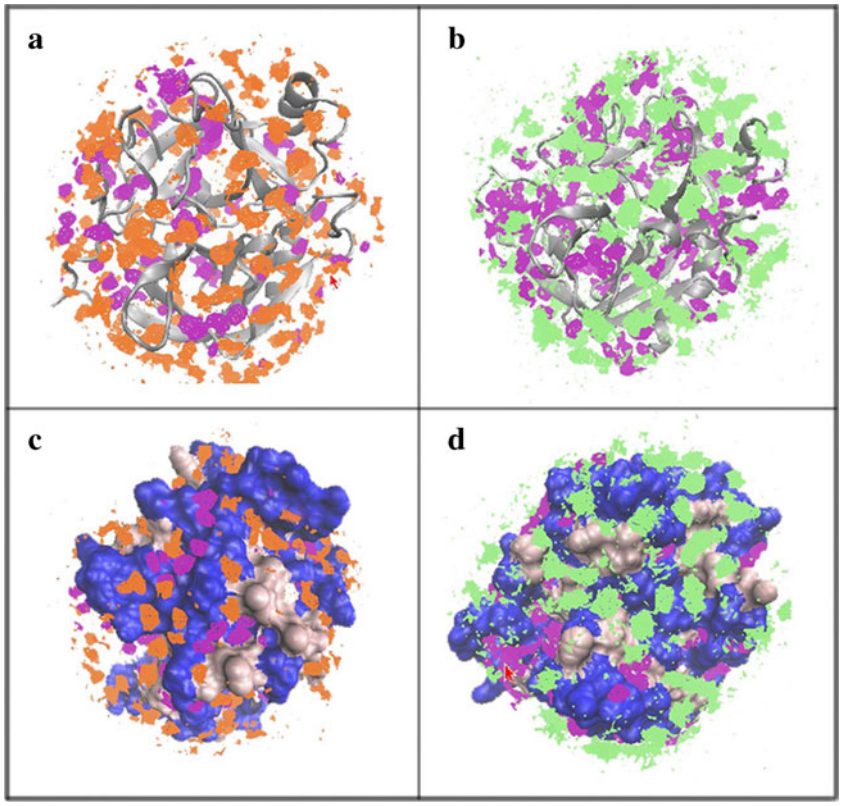

Fig. 6 The spatial density distribution of water and organic molecules around the protein in acetonitrile (**a**, **c**) and hexane (**b**, **d**) media, and the protein corresponds to the average structure of γ-chymotrypsin-trifluoromethylketone over the last 2 ns simulation, the contours enclose regions with a probability density above five times the average density for water (*purple contour*), 14 times for acetonitrile (*orange contour*), and 36 times the average density for hexane (*lime contour*). The average structure of the enzyme was drawn according to the second structure (**a**, **b**) and the hydrophobic surface area (*silver*) and the hydrophilic surface area (*blue*) (**c**, **d**)

than that in acetonitrile, consistent with the number of water molecules in the 2.5 Å region from the protein surface calculated above. In addition, Fig. 6c and d further suggest that the water molecules on the protein surface seem to be clustered mainly nearby the hydrophilic residues represented by the hydrophilic surface while the organic solvents mainly distribute nearby the hydrophobic residues represented by the hydrophobic surface.

To gain more insight into the solvent molecule distribution around the protein surface, we further calculate the concentration percentage of water molecules and organic molecules within solvation layer around protein in all hydration levels. The solvent around protein surface is partitioned into shells of 1 Å thickness. Average values of solvent molecule amount in every shell are obtained over the last 2 ns trajectories. The solvent concentration in each shell is defined as the percentage of the amount of organic solvent in each shell relative to the total amount of corresponding solvent within 12 Å. Figure 7 shows the correlation of solvent (viz., water molecules, acetonitrile, and hexane molecules) concentration with protein-to-solvent distance, which is helpful for us to extract information about intermolecular interaction and local structure of solutions and to detect aggregation phenomena in multicomponent liquid systems.

As shown in Fig. 7a and b, the acetonitrile and hexane are not evenly distributed over the protein surface. There is an organic rich solvation layer (viz., first solvation layer) at *ca.* 3 Å from protein and the location of the layer is hardly affected by different water contents. However, the water content can influence the concentration of organic solvent in the solvation layer. The concentration of organic solvent in the rich region decreases as the water content increases. As can be seen from Fig. 7, the effect of water content on the concentration of hexane in the first solvation layer is more significant than that of acetonitrile when the water content is lower than 10 %. However, when the water content is higher than 10 %, the concentration of hexane molecules in the first solvation layer changes little with continuous increase in the water content and approaches the bulk density. While for acetonitrile medium, the concentration of it in the first organic solvation layer is the highest at all hydration levels, implying that the water molecule does not completely exclude the acetonitrile molecules from the protein surface. Figure 7c and d shows that the water concentrations around the protein are not constant. The phenomenon is more pronounced in low hydration levels. For example, the water around the protein presents higher concentration relative to the bulk concentration, especially in the case of ≤10 % water content. It can be observed that the first hydration layer (viz., the highest hydration layer) locates at *ca.* 2 Å distance from protein in acetonitrile medium when the water content is lower than 20 %. Increasing water content, the highest hydration layer is postponed to *ca.* 3 Å distance and the concentration of water around the protein gradually approaches to be constant. In the case of ≥50 % water content, the distribution of water seems to be constant and close to

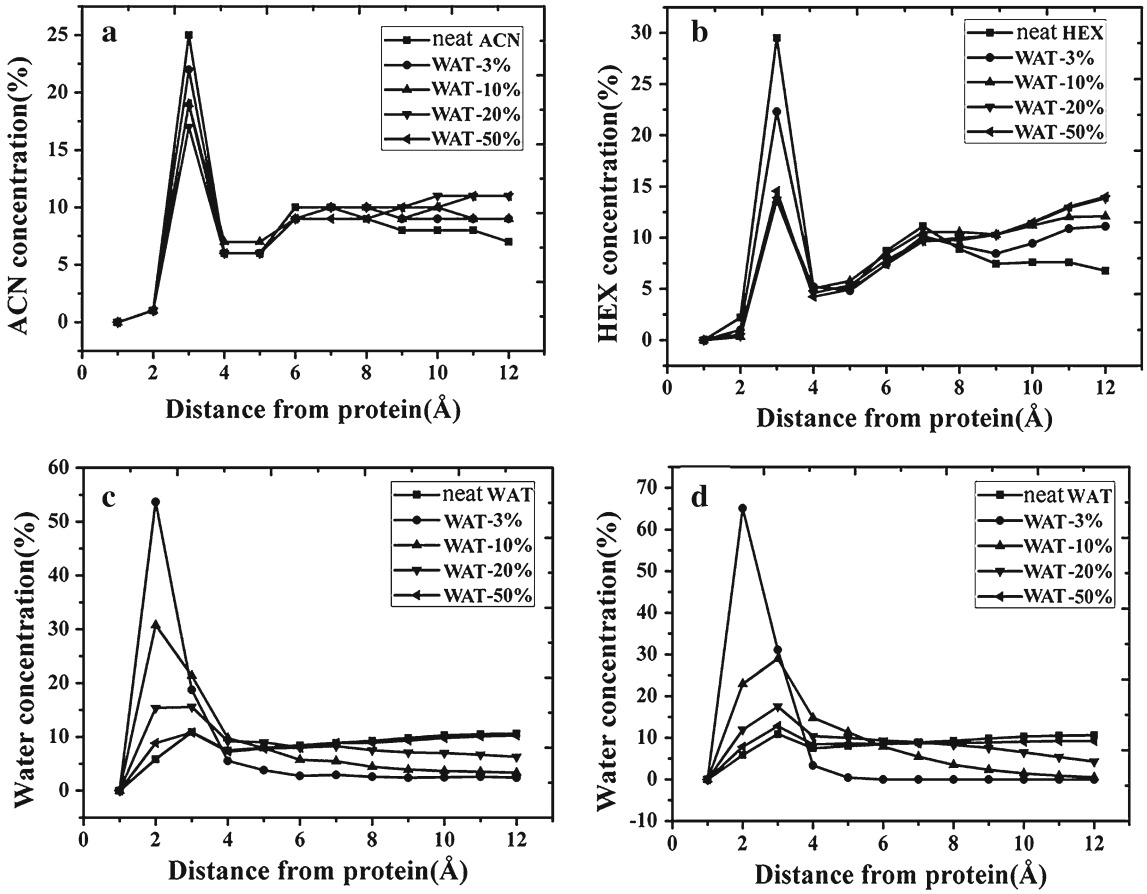

Fig. 7 The water (WAT), acetonitrile (ACN) and hexane (HEX) concentration in every shell (1 Å) within 12 Å around protein (distance in Å). The left panel (**a**, **c**) is for the acetonitrile media, and the right panel (**b**, **d**) is for the hexane media

the values of the bulk density. Similar variations are observed in hexane medium, but, with the rich hydration shell moved to~3 Å distance at lower water content (10 %).

These observations above suggest that the water molecules are mainly distributed around protein surface at the low hydration level, consistent with the spatial density distribution above. The distribution could weaken the direct interaction between the organic molecules and the protein, which should play an important role for the proteases to retain its catalytic activity in micro-hydrated polar and nonpolar solvents.

Conclusions

In this work, we select the tetrahedral complex of chymotrypsin-trifluoromethyl ketone as a model of the transition state of chymotrypsin in catalytic reaction, and employ MD method to study the effect of five water contents (3 %, 10 %, 20 %, 50 %, 100 %v/v) on its structure, solvent distribution and H-bonding in polar acetonitrile and nonpolar hexane media. Our objective is to provide some helpful information at molecular level for better understanding the effects of water content on the structure and function of enzyme in non-aqueous media.

In the time scale of the simulation, it can be observed that the calculated RMSD and RMSF values display a clear correlation with the water content in hexane medium. Namely, the RMSD of enzyme decreases with increasing water content while the RMSF displays a reverse trend. However, the correlation between these two parameters and the water content can not be observed in polar acetonitrile solvent, where the RMSD and RMSF values display to some extent U-shaped dependence on the water content with a minimum somewhere between 10 % and 20 %. A comparison of the two parameters between the two organic solvents revealed that the RMSD is lower in polar acetonitrile media than that in nonpolar hexane at<50 % water content level and the difference between the two solvents decreases with increasing water content. The RMSF value is higher in acetonitrile medium than that in hexane at low water content (<10 %), after which an opposite trend occurs for the two solvents. The reason should be attributed to the fact that there are fewer water molecules around the protein in acetonitrile medium due to its stronger ability to strip off

the water molecule than the non-polar hexane at the same water content, thus disfavoring the flexibility of protein.

The radius of gyration and solvent-accessible surface area in hexane medium are lower than those in acetonitrile at all hydration levels, suggesting that the enzyme structure in non-polar solvent is more compact than that in polar. The difference in the two parameters between the two organic media is more obvious at low water content (<10 %), after which the difference is reduced by a continuous increase in the water amount. The water content induced changes in the number of H-bonds and salt bridges could rationalize the variation trend of the SASA and the radius of gyration at different hydration levels. Namely, the greater the number of H-bonds and salt bridges, the more compact the protein structure. Judging from the SASA variation, we could assume that the hydrophobic and hydrophilic side chains both reorient themselves on the protein surface owing to changes in the water content.

H-bond analysis in the active site reveals that the water contents in the two organic solvents do not play an observable role in the stability of hydrogen-bond network between the three catalytic residues since the H-bonds present high stability at all hydration levels. The observation is different from the previous research on the free enzyme. Indeed, it is observed that the existence of trifluoromethyl ketone makes the solvent molecules (including water molecules and organic solvent molecules) hardly penetrate into active site of enzyme. It is the lack of the perturbation effects of solvent molecules in the active site that leads to high stability of the catalytic H-bond network. While for the free enzyme, there are solvent molecules penetrating into the active site and they could form H-bond with the catalytic residues, as confirmed by our previous work. Thus, the stability of the H-bond network is weakened in the free enzyme system.

Solvent distribution around the protein surface shows that an increase in the water content produces no significant effect on the location of richest solvation layer of organic solvent since their position almost retains at the 2–3 Å distance from the protein surface at all hydration levels, suggesting that the increase in the water content could not fully exclude organic molecules from the protein surface. However, it was observed that the rich layer of water is closer to protein than that of organic solvent at low hydration level. It seems that these water molecules create one coat around protein surface and exclude organic solvent within the scale of simulation time. On the whole, the organic solvent distribution around protein is not even but presents micro heterogeneity. Similar heterogeneity is observed for the distribution of water molecules at low hydration level (<10 %), where the water molecules mainly distribute near the hydrophilic residues of the protease, and the number of water molecules around the enzyme surface in hexane medium is larger than that in acetonitrile, confirming stronger ability of acetonitrile to strip off water. When the water content is higher than 50 %, the water concentration approaches to be even and is close to bulk density.

In summary, the variation trend of these calculated structure properties (*e.g.*, RMSD, RMSF, SASA, HB, *etc*.) in the organic solvents with 10~20 %v/v water content approaches, to a large extent, to those in aqueous system, providing a support for the experimental observations that there is a bell-shaped dependence on the water content or an optimal water content for the catalytic activity of some enzymes in non-aqueous media. Thus, the observations from the work could provide useful information for understanding the correlation between enzyme catalytic activity and the water content.

Acknowledgments This project is supported by the National Science Foundation of China (Grant No. 20973115, 21273154, U1230121) and the International Science and Technology Cooperation Foundation of Sichuan province (Grant No. 2011H0003).

References

1. Gupta MN, Roy I (2004) Enzymes in organic media. Eur J Biochem 271(13):2575–2583
2. Klibanov AM (2001) Improving enzymes by using them in organic solvents. Nature 409(6817):241–246
3. Cabral JMS, Aires-Barros MR, Pinheiro H, Prazeres DMF (1997) Biotransformation in organic media by enzymes and whole cells. J Biotechnol 59(1–2):133–143
4. Partridge J, Moore BD, Halling PJ (1999) α-Chymotrypsin stability in aqueous-acetonitrile mixtures: is the native enzyme thermodynamically or kinetically stable under low water conditions? J Mol Catal B Enzym 6(1–2):11–20
5. Anthonsen T, Sjurnes BJ (2000) In: Gupta MN (ed) Methods in Nonaqueous Enzymology. Birkhäuser, Basel
6. Castro GR (2000) Properties of soluble α-chymotrypsin in neat glycerol and water. Enzym Microb Technol 27(1–2):143–150
7. Simon LM, Kotormán M, Maráczi K, László K (2000) N-acetyl-l-arginine ethyl ester synthesis catalysed by bovine trypsin in organic media. J Mol Catal B Enzym 10(6):565–570
8. Soares CM, Teixeira VH, Baptista AM (2003) Protein structure and dynamics in nonaqueous solvents: insights from molecular dynamics simulation studies. Biophys J 84(3):1628–1641
9. Clark DS (2004) Characteristics of nearly dry enzymes in organic solvents: implications for biocatalysis in the absence of water. Philos Trans R Soc Lond B 359(1448):1299–1307
10. Diaz-Vergara N, Piñeiro Á (2008) Molecular dynamics study of triosephosphate isomerase from trypanosoma cruzi in water/decane mixtures. J Phys Chem B 112(11):3529–3539
11. Hudson EP, Eppler RK, Clark DS (2005) Biocatalysis in semi-aqueous and nearly anhydrous conditions. Curr Opin Biotechnol 16(6):637–643
12. Branco RJF, Graber M, Denis V, Pleiss J (2009) Molecular mechanism of the hydration of candida antarctica lipase B in the gas phase: water adsorption isotherms and molecular dynamics simulations. ChemBioChem 10(18):2913–2919
13. Kijima T, Yamamoto S, Kise H (1996) Study on tryptophan fluorescence and catalytic activity of α-chymotrypsin in aqueous-organic media. Enzym Microb Technol 18(1):2–6
14. Simon LM, Kotormán M, Garab G, Laczkó I (2001) Effects of polyhydroxy compounds on the structure and activity of α-chymotrypsin. Biochem Biophys Res Commun 293(1):416–420

15. Luo Q, Han WW, Zhou YH, Li ZS (2008) The 3D structure of the defense-related rice protein Pir7b predicted by homology modeling and ligand binding studies. J Mol Model 14(7):559–569
16. Da LT, Wang D, Huang X (2012) Dynamics of pyrophosphate lon release and its coupled trigger loop motion from closed to open state in RNA polymerase II. J Am Chem Soc 134(4):2399–2406
17. Yang MJ, Pang XQ, Zhang X, Han KL (2011) Molecular dynamics simulation reveals preorganization of the chloroplast FtsY towards complex formation induced by GTP binding. J Struct Biol 173(1):57–66
18. Wu R, Xie H, Cao Z, Mo Y (2008) Combined quantum mechanics/molecular mechanics study on the reversible isomerization of glucose and fructose catalyzed by pyrococcus furiosus phosphoglucose isomerase. J Am Chem Soc 130(22):7022–7031
19. Toba S, Hartsough DS (1996) Solvation and dynamics of chymotrypsin in hexane. J Am Chem Soc 118(27):6490–6498
20. Micaelo NM, Teixeira VH, Baptista AM, Soares CM (2005) Water dependent properties of cutinase in nonaqueous solvents: a computational study of enantioselectivity. Biophys J 89(2):999–1008
21. Micaelo NM, Soares CM (2007) Modeling hydration mechanisms of enzymes in nonpolar and polar organic solvents. FEBS J 274(9):2424–2436
22. Rezaei-Ghaleh N, Amininasab M, Nemat-Gorgani M (2008) Conformational changes of α-chymotrypsin in a fibrillation-promoting condition: a molecular dynamics study. Biophys J 95(9):4139–4147
23. Yang L, Dordick JS, Garde S (2004) Hydration of enzyme in nonaqueous media is consistent with solvent dependence of its activity. Biophys J 87(2):812–821
24. Trodler P, Pleiss J (2008) Modeling structure and flexibility of candida Antarctica lipase B in organic solvents. BMC Struct Biol 8:9
25. Li C, Tan T, Zhang H, Feng W (2010) Analysis of the conformational stability and activity of candida antarctica lipase B in organic solvents. J Biol Chem 285(37):28434–28441
26. Wedberg R, Abildskov J, Peters GH (2012) Protein dynamics in organic media at varying water activity studied by molecular dynamics simulation. J Phys Chem B 116(8):2575–2585
27. Jing YQ, Han KL (2010) Quantum mechanical effect in protein-ligand interaction. Expert Opin Drug Discov 5(1):33–49
28. Li DM, Wang Y, Han KL (2012) Recent density functional theory model calculations of drug metabolism by cytochrome P450. Coord Chem Rev 256(11–12):1137–1150
29. Hedstrom L (2002) Serine protease mechanism and specificity. Chem Rev 102(12):4501–4523
30. Westler WM, Weinhold F, Markley JL (2002) Quantum Chemical Calculations on Structural Models of the Catalytic Site of Chymotrypsin: Comparison of Calculated Results with Experimental Data from NMR Spectroscopy. J Am Chem Soc 124(48):14373–14381
31. Molina PA, Jensen JH (2003) A predictive model of strong hydrogen bonding in proteins: the Nδ1−H−Oδ1 hydrogen bond in low-pH α-chymotrypsin and α-lytic protease. J Phys Chem B 107(25):6226–6233
32. Ishida T, Kato S (2003) Theoretical perspectives on the reaction mechanism of serine proteases: the reaction free energy profiles of the acylation process. J Am Chem Soc 125(39):12035–12048
33. Shokhen M, Albeck A (2004) Is there a weak H-bond→LBHB transition on tetrahedral complex formation in serine proteases? Proteins: Struct Funct Bioinf 54(3):468–477
34. Topf M, Richards WG (2004) Theoretical studies on the deacylation step of serine protease catalysis in the gas phase, in solution, and in elastase. J Am Chem Soc 126(44):14631–14641
35. Shokhen M, Khazanov N, Albeck A (2007) The cooperative effect between active site ionized groups and water desolvation controls the alteration of acid/base catalysis in serine proteases. ChemBioChem 8(12):1416–1421
36. Case DA, Darden TA, Cheatham TE, Simmerling CL, Wang J, Duke RE, Luo R, Crowley M, Walker RC, Zhang W, Merz KM, Wang B, Hayik S, Roitberg A, Seabra G, Kolossvary I, Wong KF, Paesani F, Vanicek J, Wu X, Brozell SR, Steinbrecher T, Gohlke H, Yang L, Tan C, Mongan J, Hornak V, Cui G, Mathews DH, Seetin MG, Sagui C, Babin V, Kollman PA (2008) Amber 10, 10th edn. University of California San Francisco, San Francisco
37. Duan Y, Wu C, Chowdhury S, Lee MC, Xiong G, Zhang W, Yang R, Cieplak P, Luo R, Lee T, Caldwell J, Wang J, Kollman P (2003) A point-charge force field for molecular mechanics simulations of proteins based on condensed-phase quantum mechanical calculations. J Comput Chem 24(16):1999–2012
38. Jorgensen WL, Chandrasekhar J, Madura JD, Impey RW, Klein ML (1983) Comparison of simple potential functions for simulating liquid water. J Chem Phys 79(2):926–935
39. Wang J, Wolf RM, Caldwell JW, Kollman PA, Case DA (2004) Development and testing of a general amber force field. J Comput Chem 25(9):1157–1174
40. Wang J, Wang W, Kollman PA, Case DA (2006) Automatic atom type and bond type perception in molecular mechanical calculations. J Mol Graph Model 25(2):247–260
41. Brady K, Wei A, Ringe D, Abeles RH (1990) Structure of chymotrypsin-trifluoromethyl ketone inhibitor complexes: comparison of slowly and rapidly equilibrating inhibitors. Biochemistry 29(33):7600–7607
42. Berendsen HJC, Postma JPM, Van Gunsteren WF, DiNola A, Haak JR (1984) Molecular dynamics with coupling to an external bath. J Chem Phys 81(8):3684–3690
43. Ryckaert JP, Ciccotti G, Berendsen HJC (1977) Numerical integration of the cartesian equations of motion of a system with constraints: molecular dynamics of n-alkanes. J Comput Phys 23(3):327–341
44. Darden T, York D, Pedersen L (1993) Particle mesh ewald: an N-log(N) method for ewald sums in large systems. J Chem Phys 98(12):10089–10092
45. Essmann U, Perera L, Berkowitz ML, Darden T, Lee H, Pedersen LG (1995) A smooth particle mesh Ewald method. J Chem Phys 103(19):8577–8593
46. Ulbert O, Bélafi-Bakó K, Tonova K, Gubicza L (2005) Thermal stability enhancement of Candida rugosa lipase using ionic liquids. Biocatal Biotransform 23(3–4):177–183
47. Ulbert O, Fráter T, Bélafi-Bakó K, Gubicza L (2004) Enhanced enantioselectivity of Candida rugosa lipase in ionic liquids as compared to organic solvents. J Mol Catal B Enzym 31(1–3):39–45
48. Zhu L, Yang W, Meng YY, Xiao X, Guo Y, Pu X, Li M (2012) Effects of organic solvent and crystal water on γ-chymotrypsin in acetonitrile media: observations from molecular dynamics simulation and DFT calculation. J Phys Chem B 116(10):3292–3304
49. Nakagawa S, Yu HA, Karplus M, Umeyama H (1993) Active site dynamics of acyl-chymotrypsin. Proteins: Struct Funct Bioinf 16(1):172–194
50. Kuszewski J, Gronenborn AM, Clore GM (1999) Improving the packing and accuracy of NMR structures with a pseudopotential for the radius of gyration. J Am Chem Soc 121(10):2337–2338
51. Copeland RA (2000) Enzymes: a practical introduction to structure, mechanism, and data analysis. Wiley, New York
52. Humphrey W, Dalke A, Schulten K (1996) VMD: visual molecular dynamics. J Mol Graphics 14(1):33–38